

Mechanism of Gas Transport in Plasma Treated Glassy Polymer Films

E. SADA, H. KUMAZAWA, P. XU, and T. KIYOHARA,
*Department of Chemical Engineering, Kyoto University,
Kyoto 606, Japan*

Synopsis

The effect of oxygen- and Ar-plasma treatment on glassy polysulfone and polyimide films upon the gas diffusion process was investigated in the permeation of CO₂ and H₂. The plasma treatment apparently induced a reduction of only the diffusivity of Henry's law population, while the diffusion coefficient of the Langmuir population was not altered by plasma treatment. The oxygen- and Ar-plasma treatment on polysulfone films is favorable for permselectivity of H₂ relative to CO₂. Such a surface modification of polyimide films appears to be ineffective for improvement of permselectivity of H₂.

INTRODUCTION

It has been expected that the surface modification of gas separation membrane by plasma treatment induces an increase in the permselectivity of smaller gas molecules such as H₂ and He relative to larger gas molecules, because the surface treatment forms crosslinked networks in the neighborhood of the membrane surface. The plasma treatment has been believed to have an influence only on the diffusion process, and macroscopically the retardation of the diffusivity as a lumped parameter has been measured. In the glassy polymer membranes, where two kinds of population execute diffusive movements, how the plasma treatment affects the respective modes of diffusion is an interesting subject.

In the present research, one aim is to elucidate the effect of oxygen- and argon-plasma treatment on glassy polymer films upon the diffusion process of carbon dioxide and hydrogen. Polysulfone and polyimide films, both of which have an excellent property of highly chemical and thermal stability, were employed as the glassy polymer film. The effects of plasma treatment on the diffusion processes of Henry's law and Langmuir modes have been estimated from permeability measurements. Another aim in this research is to discuss the degree of improvement of permselectivity of H₂ relative to CO₂ induced by such a surface modification.

THEORETICAL BACKGROUND

The dual-mode sorption and mobility model, which is conventionally employed to simulate sorption and permeation behavior of a gas in glassy polymer films, is briefly described.

The dual-mode sorption model postulates two simultaneous sorption modes comprising a normal Henry's law dissolution in the polymer matrix and a

Langmuir adsorption in preexisting unrelaxed microvoids. Quantitatively, this may be written as

$$C = C_D + C_H = k_D p + C'_H b p / (1 + b p) \quad (1)$$

In the dual-mode mobility model, two kinds of steady-state permeation flux have been presented in terms of gradients of concentration¹ and chemical potential.² The mean permeability coefficient in terms of the proportionality to the concentration gradient has been derived by Paul and Koros:¹

$$\bar{P} = k_D D_D + \frac{C'_H b D_H}{(1 + b p_1)(1 + b p_2)} \quad (2)$$

The above equation states that the mean permeability coefficient \bar{P} should be linear to the term $b/(1 + b p_1)(1 + b p_2)$.

On the other hand, the mean permeability coefficient expression in terms of the proportionality to the chemical potential gradient has been derived by Petropoulos:²

$$\bar{P} = k_D D_D + \frac{C'_H D_H}{p_2 - p_1} \ln \frac{1 + b p_2}{1 + b p_1} \quad (3)$$

It suggests that the mean permeability coefficient \bar{P} and the term

$$\frac{1}{p_2 - p_1} \ln \frac{1 + b p_2}{1 + b p_1}$$

should give a linear relationship.

EXPERIMENTAL

Equilibria of H₂ by polysulfone (hereafter PSF) and polyimide (hereafter PI) film samples and of CO₂ by PI were measured by the pressure decay method.³ The sorption cell is similar to one designed by Koros et al.,⁴ and the pressure in the sorption cell was continuously monitored by a pressure transducer. The permeabilities of CO₂ and H₂ through both the film samples with and without oxygen- and Ar-plasma dose were measured by the variable-volume method employed by Stern et al.⁵ The gas to be permeated was fed into the upstream side, while the downstream side was filled with the same gas at 0.101 MPa. Hence, the downstream pressure is always kept constant at 0.101 MPa. The volumetric flow rate through the film to the downstream side was measured by observing the displacement of a small amount of 1-propanol in a capillary tube connected to the downstream-pressure side. The mean permeability coefficient was determined from this steady-state permeation rate. The permeation area of the cell was 19.6 cm².

The PSF film samples (Torayslon-PS) were kindly supplied by Toray Co. Ltd., Japan. The glass transition temperature has been reported to be 190°C by Toray. The thickness of the film used was 50 μm. The PI film samples (Kapton 100H) were kindly supplied also by Toray-DuPont Co. Ltd., Japan.

The sample is a glassy material with a glass transition temperature above 350°C. The thickness of the film used was 25 μm .

The plasma treatment was conducted in a flow-type cylindrical reactor with external plate electrode (Yamato, PR-510A). The inner diameter and length of the reactor are 21.5 and 27.5 cm, respectively. It is similar to one reported by Hollahan and Bell.⁶ The glow discharge was generated under a pressure of 0.2 Torr at a frequency of 13.56 MHz, and the electric power of discharge was kept constant at 100 W. Oxygen or argon was used for a plasma gas. The flow rates of oxygen and Ar were maintained at 3 and 10 cm^3/min , respectively. The exposure time was varied from 5 to 20 min for treatment on PSF films and from 5 to 40 min for treatment on PI films.

RESULTS AND DISCUSSION

Sorption Equilibria

The sorption isotherms for CO_2 in PSF film at four levels of temperature between 30 and 45°C were measured in our work.⁷ The isotherm could be simulated well in terms of the dual-mode sorption model, eq. (1), and the dual-mode sorption parameters were determined as listed in Table I. In the same table, the dual-mode sorption parameters for the same systems previously measured^{8,9} were listed. The values of the Langmuir affinity constant b are different from the earlier studies.^{8,9} The difference may be explained in terms of possible differences in sample histories, sample production methods, and additives.

The measured sorption isotherms for the same gas in PI film at 30, 40, and 60°C are demonstrated in Figure 1. Each isotherm exhibits a nonlinear pattern similar to those observed for PSF⁷ and other glassy polymers.^{3,10} Similarly, the sorption behavior could be described adequately by the dual-

TABLE I
Sorption Parameters for CO_2 and H_2 in PSF Film

Temp (°C)	k_D [$\text{cm}^3(\text{STP})/\text{cm}^3 \text{atm}$]	b (atm^{-1})	C_H' [$\text{cm}^3(\text{STP})/\text{cm}^3$]
	<u>CO_2-PSF</u>		
30	0.646	0.195	20.5
35	0.595	0.178	19.4
40	0.547	0.168	18.3
45	0.508	0.155	17.1
	<u>CO_2-PSF⁸</u>		
35	0.664	0.326	17.9
	<u>CO_2-PSF⁹</u>		
20	0.801	0.410	26.0
35	0.725	0.390	19.2
65	0.231	0.134	17.5
	<u>H_2-PSF</u>		
30	0.120	—	—
40	0.104	—	—
50	0.085	—	—

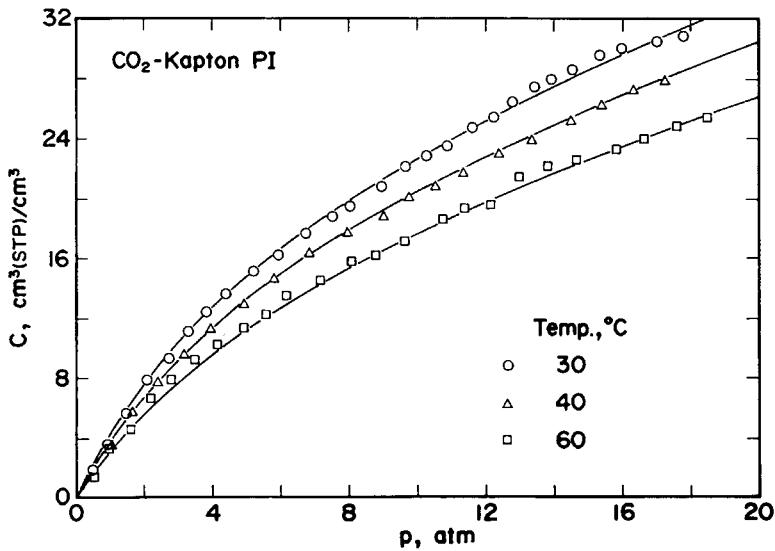


Fig. 1. Sorption isotherms for CO_2 in PI (Kapton 100H) film at different temperatures ($^{\circ}\text{C}$): (○) 30; (△) 40; (□) 60.

mode sorption model. The values of the dual-mode sorption parameters were determined by a nonlinear-least-square method and are listed in Table II. The solid curves in Figure 1 represent the sorption isotherms calculated using eq. (1) and these estimates. In Table II, the dual-mode sorption parameters for CO_2 in 0.3-mil Kapton polyimide film measured by Chern et al.¹¹ were listed. The values of b are different from this earlier study¹¹ possibly due to the similar reasons described above.

The measured sorption isotherms for H_2 in PSF and PI films at 30, 40, and 50 $^{\circ}\text{C}$ are shown in Figures 2 and 3. Each isotherm exhibits negligible curvature and can be described well by Henry's law, viz.,

$$C = k_D p \quad (4)$$

TABLE II
Sorption Parameters for CO_2 and H_2 in PI Film

Temp ($^{\circ}\text{C}$)	k_D [$\text{cm}^3(\text{STP})/\text{cm}^3 \text{ atm}$]	b (atm^{-1})	C'_H [$\text{cm}^3(\text{STP})/\text{cm}^3$]
<u>CO_2-PI</u>			
30	0.715	0.161	25.2
40	0.651	0.151	23.3
60	0.635	0.145	19.1
<u>CO_2-PI¹¹</u>			
60	0.380	0.296	12.5
<u>H_2-PI</u>			
30	0.243	—	—
40	0.192	—	—
50	0.156	—	—

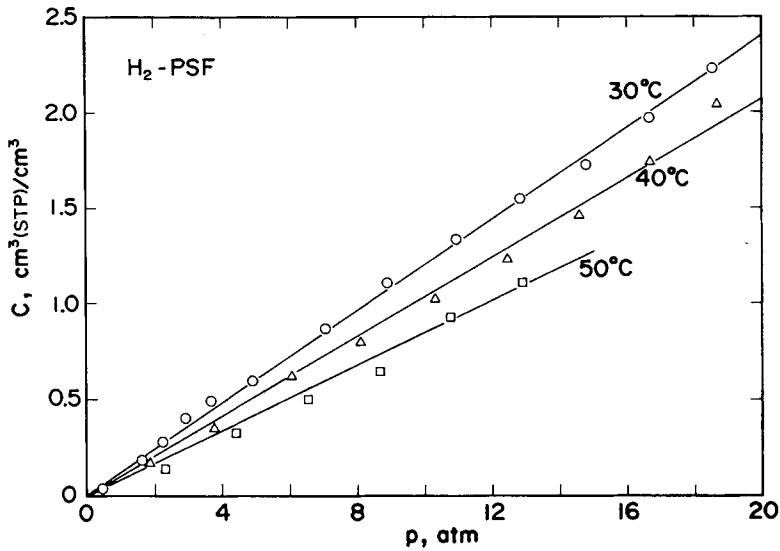


Fig. 2. Sorption isotherms for H_2 in PSF film at different temperatures ($^{\circ}C$): (\circ) 30; (Δ) 40; (\square) 50.

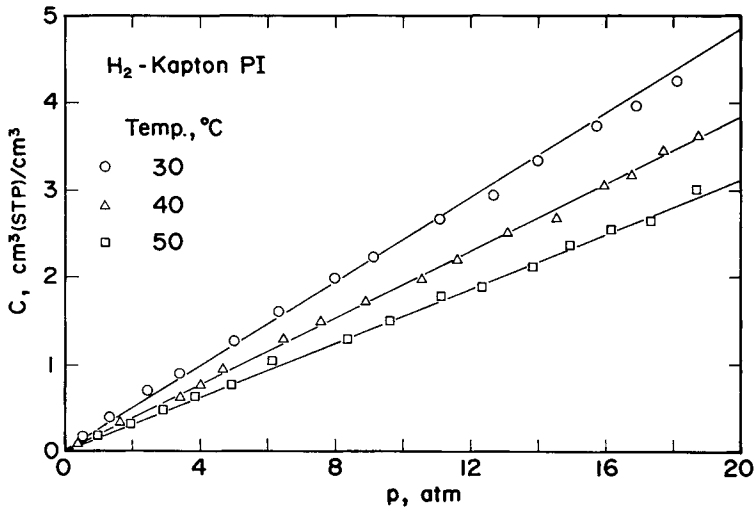


Fig. 3. Sorption isotherms for H_2 in PI film at different temperatures ($^{\circ}C$): (\circ) 30; (Δ) 40; (\square) 50.

The Henry's law constants calculated from the slopes were listed in Tables I and II.

Permeabilities of CO_2 and H_2 in Oxygen-Plasma-Treated PSF and PI Films

First, the experimental results of mean permeability coefficients of CO_2 through untreated PSF film are illustrated as a function of upstream pressure in Figure 4. At every temperature, the permeability coefficients decreased with

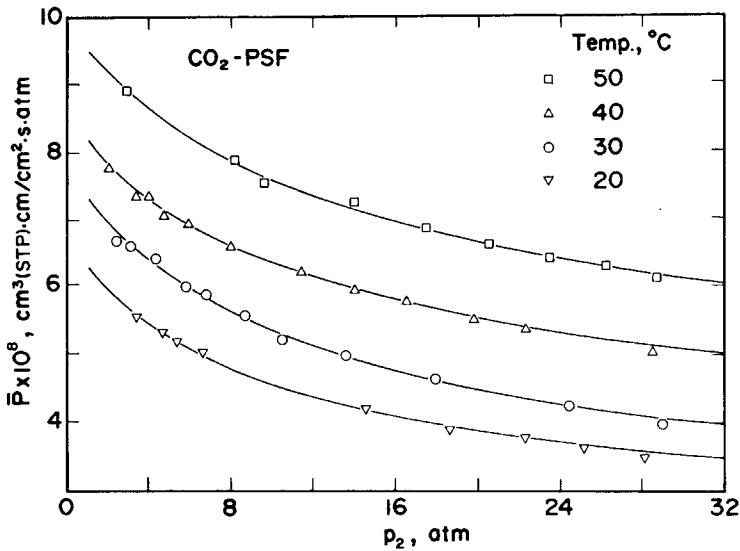


Fig. 4. Effect of upstream pressure on mean permeability coefficient of CO₂ in PSF film at different temperatures (°C): (□) 50; (Δ) 40; (○) 30; (▽) 20.

increasing upstream pressure, characteristic of glassy polymers. Then, it was examined whether the dual-mode mobility model driven by gradients of concentration or chemical potential was applicable.

The mean permeability coefficient data were plotted on the basis of eqs. (2) and (3), respectively, in Figures 5 and 6. The plots in Figure 5 did not give any straight lines at all temperatures covered, whereas the plots in terms of eq. (3) depicted in Figure 6 gave essentially straight lines. It implies that the dual-mode mobility model driven by gradients of chemical potential is applicable to this system. From the slope and intercept of each straight line in Figure 6, the diffusion coefficients D_D and D_H were determined, and the temperature dependencies of these two diffusion coefficients were indicated as an Arrhenius plot in Figure 7. The values of the diffusion coefficients D_D and D_H for a similar system had been measured at 35°C by Erb and Paul⁸ and Maeda and Paul.⁹ The values of D_D in the present study are close to those reported in these two earlier studies, whereas the values of D_H are much larger (about four times larger) than those in the earlier studies. The difference may be also explained in terms of possible differences in sample histories, sample production methods, and additives. Further, it is due to the differences in sorption equilibria, specifically, Langmuir affinity constants. For the sake of comparison, the present permeability coefficient data at 40°C were plotted on the basis of both eqs. (2) and (3) using the value of b reported by Maeda and Paul⁹ ($b = 0.36 \text{ atm}^{-1}$ at 40°C). The plots are shown in Figure 8. Similarly, the dual-mode mobility model driven by gradients of chemical potential rather than concentration is applicable to this system.

The permeabilities of CO₂ through oxygen-plasma-treated PSF films at different durations of exposure are shown in Figure 9, where the mean permeability coefficients are plotted on the basis of eq. (3). The permeability was gradually decreased with an increase in exposure time. This figure shows

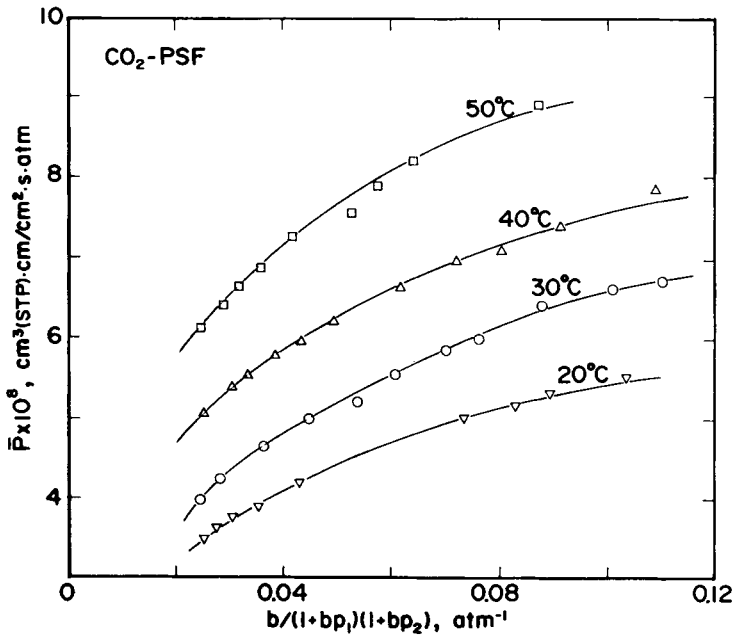


Fig. 5. Test of dual-mode mobility model driven by gradients of concentration for CO₂-PSF film.

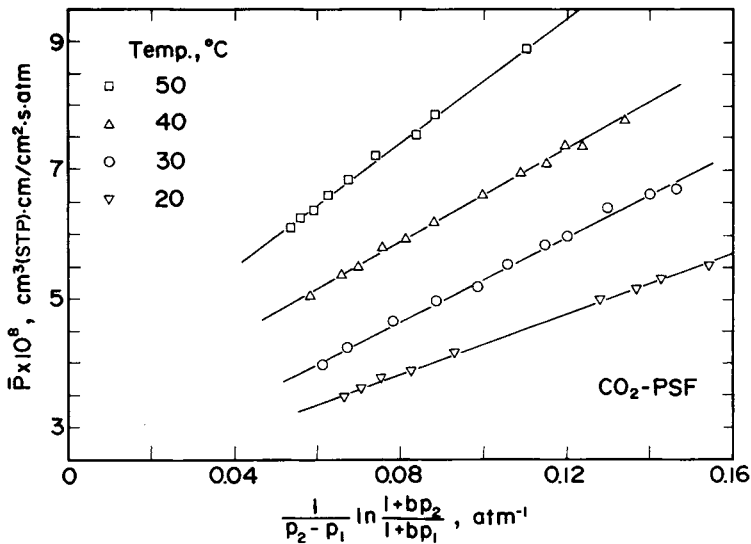


Fig. 6. Test of dual-mode mobility model driven by gradients of chemical potential for CO₂-PSF film. Temperatures (°C): (□) 50; (Δ) 40; (○) 30; (▽) 20.

that the dual-mode mobility model driven by gradients of chemical potential can be applicable also to oxygen-plasma-treated films. Though the dual-mode mobility model in itself should work well only for homogeneous dense films, it works well for the treated films as well. In the following, then, the reason will be considered.

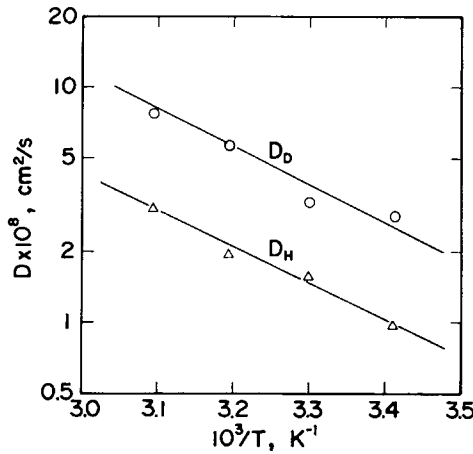


Fig. 7. Temperature dependencies of diffusion coefficients of Henry's Law and Langmuir modes for CO₂ in PSF film.

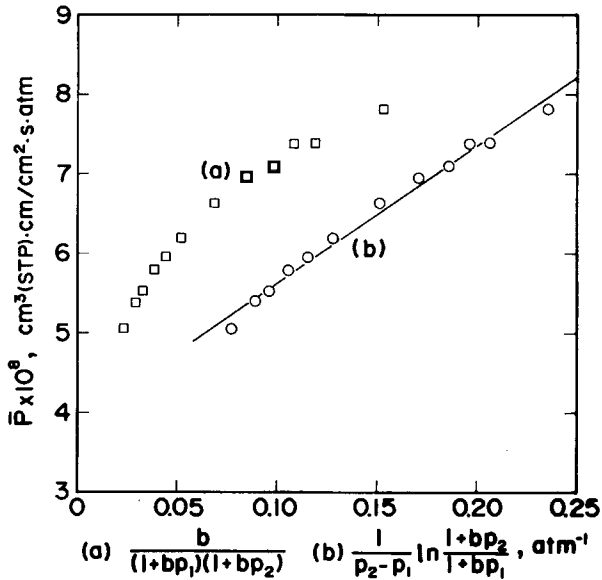


Fig. 8. Test of dual-mode mobility model using the Langmuir affinity constant reported by Maeda and Paul.⁹

The plasma treated film can be approximated by a composite structure composing of a thin surface layer treated by plasma and a remaining base polymer layer, as illustrated in Figure 10. At steady state, the permeation rate through the thin surface layer of thickness l_2 is equal to that through the base-polymer layer of thickness $l_1 (= l - l_2)$. Let the pressures of a penetrant gas on the upstream and downstream sides of this composite film be designated by p_2 and p_1 , respectively, and the pressure in between these two layers replaced by p_i .

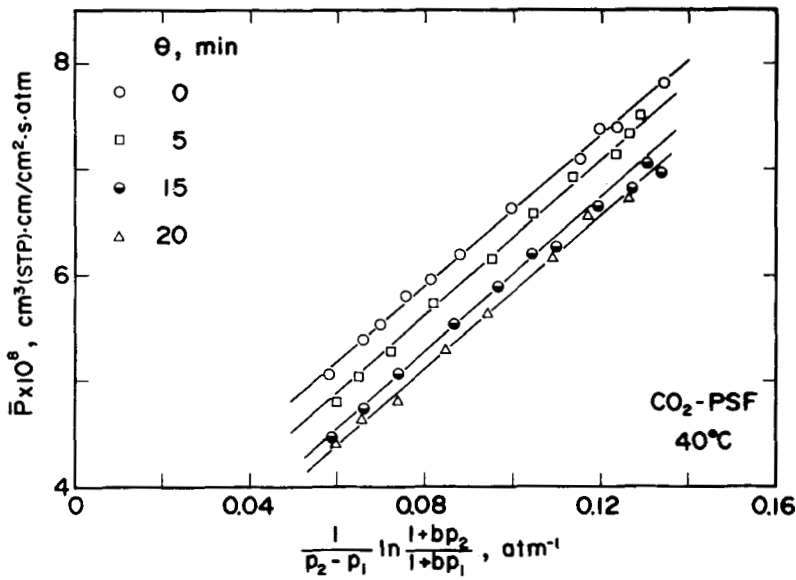


Fig. 9. Test of dual-mode mobility model driven by gradients of chemical potential for CO₂-oxygen-plasma treated PSF film at different durations (min) of treatment: (○) 0; (□) 5; (●) 15; (△) 20.

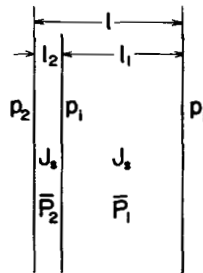


Fig. 10. Conceptual sketch of plasma treated film.

The permeation rate at steady state is written as

$$J_s = \bar{P}_2(p_2 - p_i)/l_2 = \bar{P}_1(p_i - p_1)/l_1 \tag{5}$$

where \bar{P}_2 and \bar{P}_1 refer to the mean permeability coefficients through a plasma-treated layer and an untreated base-polymer layer, respectively, and can be given by

$$\bar{P}_1 = k_D D_D + \frac{D_H C'_H}{p_i - p_1} \ln \frac{1 + bp_i}{1 + bp_1} \tag{6}$$

$$\bar{P}_2 = k_D D'_D + \frac{D'_H C'_H}{p_2 - p_i} \ln \frac{1 + bp_2}{1 + bp_i} \tag{7}$$

In eq. (7), D'_D and D'_H designate the diffusion coefficients of Henry's law and Langmuir populations in the plasma-treated layer. The permeation rate can be also given in terms of the mean permeability coefficient through a composite film (\bar{P}) as

$$J_s = \bar{P}(p_2 - p_1)/(l_2 + l_1) \quad (8)$$

From eq. (5), the following equation holds:

$$J_s = \frac{\bar{P}_2(p_2 - p_i) + \bar{P}_1(p_i - p_1)}{l_2 + l_1} \quad (9)$$

By combining eq. (9) with eq. (8), the mean permeability coefficient \bar{P} can be derived as follows:

$$\begin{aligned} \bar{P} = k_D \frac{(p_2 - p_i)D'_D + (p_i - p_1)D_D}{p_2 - p_1} \\ + \frac{D'_H C'_H}{p_2 - p_1} \ln \frac{1 + bp_2}{1 + bp_i} \\ + \frac{D_H C'_H}{p_2 - p_1} \ln \frac{1 + bp_i}{1 + bp_1} \end{aligned} \quad (10)$$

From the experimental evidence in Figure 9 that the mean permeability coefficient through plasma-treated films varies in a linear way with the term $\ln[(1 + bp_2)/(1 + bp_1)]$ and the slope of the straight line remains unchanged regardless of plasma exposure time, D'_H is believed to be equal to D_H . Equation (10) is reduced to

$$\bar{P} = k_D \left[\frac{(p_2 - p_i)D'_D + (p_i - p_1)D_D}{p_2 - p_1} \right] + \frac{D_H C'_H}{p_2 - p_1} \ln \frac{1 + bp_2}{1 + bp_1} \quad (11)$$

In the above equation, the bracketed term of the right-hand side implies a mean diffusion coefficient of Henry's law population in a composite film, which is a function of p_2 . That is,

$$\bar{P} = k_D \bar{D}_D + \frac{D_H C'_H}{p_2 - p_1} \ln \frac{1 + bp_2}{1 + bp_1} \quad (12)$$

Figure 9 shows that the plots for treated as well as untreated films exhibit straight lines parallel to each other and the intercept of the ordinate which is given by $k_D \bar{D}_D$ is affected only by the plasma exposure time. Apparently, a mean value over upstream pressures covered, \bar{D}_D , is expected to be constant with an experimental error.

From the slope and intercept of each straight line in Figure 9, the diffusion coefficients D_H and \bar{D}_D were determined. They were plotted against plasma

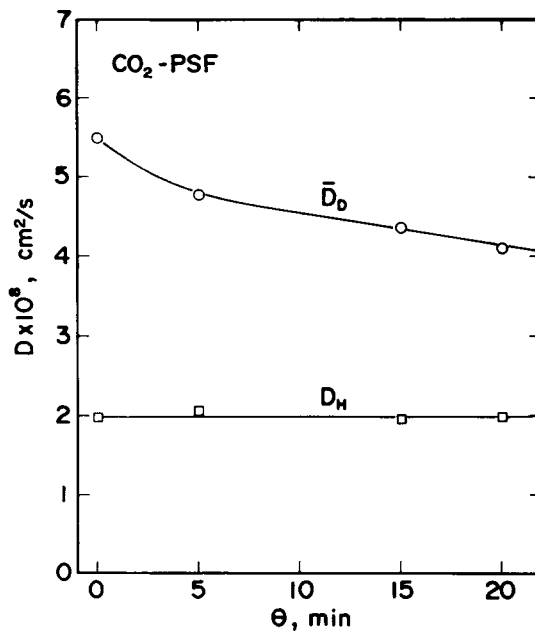


Fig. 11. Diffusion coefficients of Henry's law and Langmuir modes for CO_2 in oxygen-plasma treated PSF film at different durations of treatment.

exposure time in Figure 11. It was apparent that \bar{D}_D decreased with an increase in the exposure time (Θ), while D_H was almost independent of Θ . It suggests that the plasma treatment has an influence on the diffusion process of Henry's law dissolution population but not on that of the Langmuir adsorption population.

The pressure dependencies of the mean permeability coefficients of H_2 in oxygen-plasma-treated PSF films were demonstrated in Figure 12. As a reference, the same relationship for an untreated PSF film was also shown. The permeabilities are found to be independent of upstream pressure. By taking account this experimental evidence along with Henry-type sorption isotherms as shown in Figure 2, the permeability expression reduces to

$$\bar{P} = k_D D_D \quad (13)$$

for an untreated film, and

$$\bar{P} = k_D \frac{(p_2 - p_i)D'_D + (p_i - p_1)D_D}{p_2 - p_1} = k_D \bar{D}_D \quad (14)$$

for a treated film.

The permeability was decreased a little with an increase in plasma exposure time. The permeability data were converted to diffusivities \bar{D}_D by use of eq. (14), and \bar{D}_D was plotted against exposure time in Figure 13. In a 20-min oxygen-plasma-treated PSF film, the diffusivity \bar{D}_D of H_2 is decreased only by 4%, while that of CO_2 is reduced by 23%, as shown in Figure 14. The

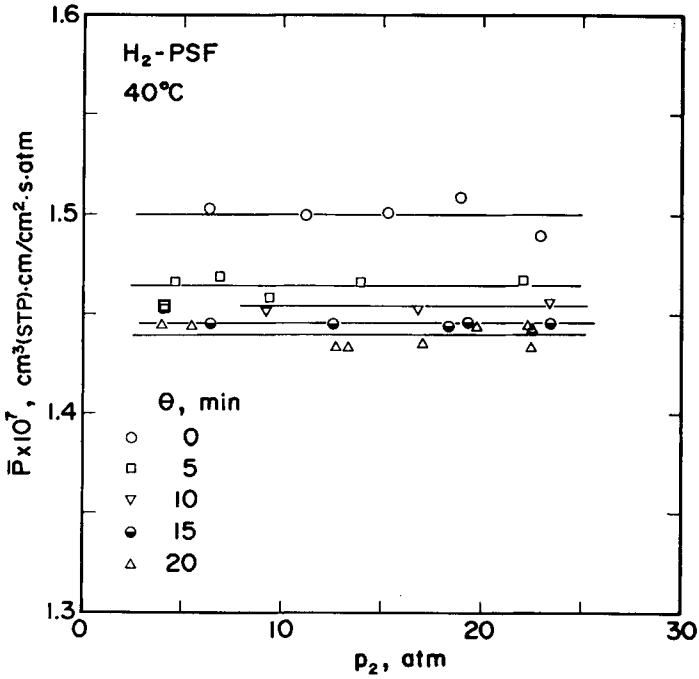


Fig. 12. Permeability coefficients for H₂ in PSF film with and without oxygen-plasma treatment.

oxygen-plasma treatment on PSF films does not have much influence on H₂ permeation. The crosslinked structure near the polymer surface induced by oxygen-plasma treatment seems to present negligible resistance to diffusion of low molecular weight gas. Therefore, the oxygen-plasma treatment on PSF films is favorable for permselectivity of H₂ relative to CO₂.

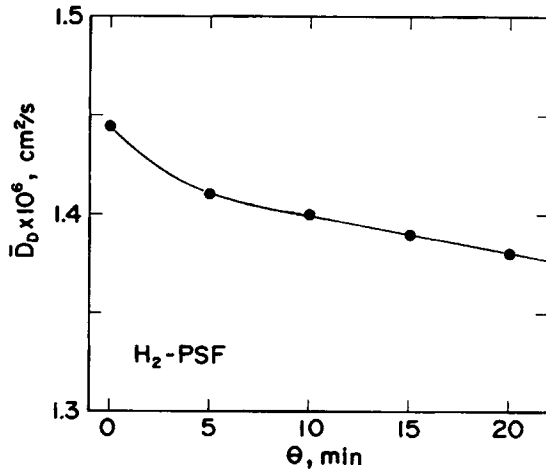


Fig. 13. Diffusion coefficients of H₂ in oxygen-plasma treated PSF film as a function of duration of treatment.

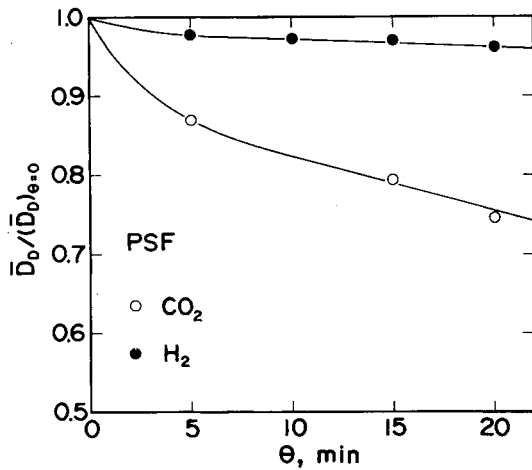


Fig. 14. Effect of duration of treatment on diffusion coefficients of CO₂ (○) and H₂ (●) in oxygen-plasma treated PSF film.

The effect of oxygen-plasma treatment on PI films, which have a more rigid structure and a higher glass transition temperature than PSF films, upon permeation behavior will be discussed below.

Measured permeability coefficients of CO₂ in an untreated PI film are illustrated on the basis of eq. (2) in Figure 15. The dual-mode mobility model driven by gradients of concentration is not operative as in case of PSF films.

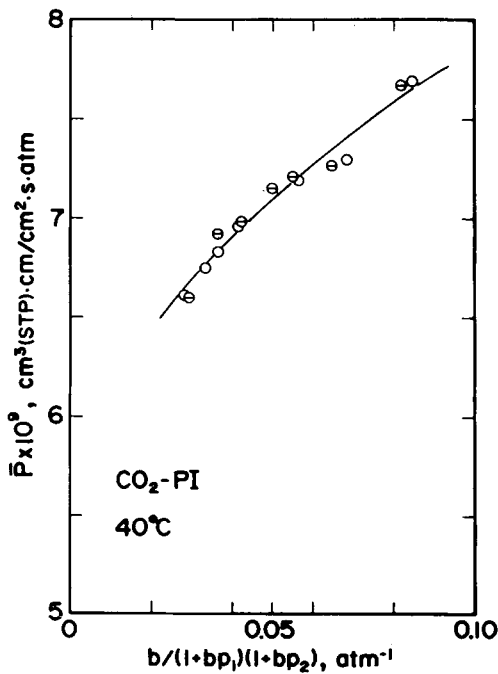


Fig. 15. Test of dual-mode mobility model driven by gradients of concentration for CO₂-PI film.

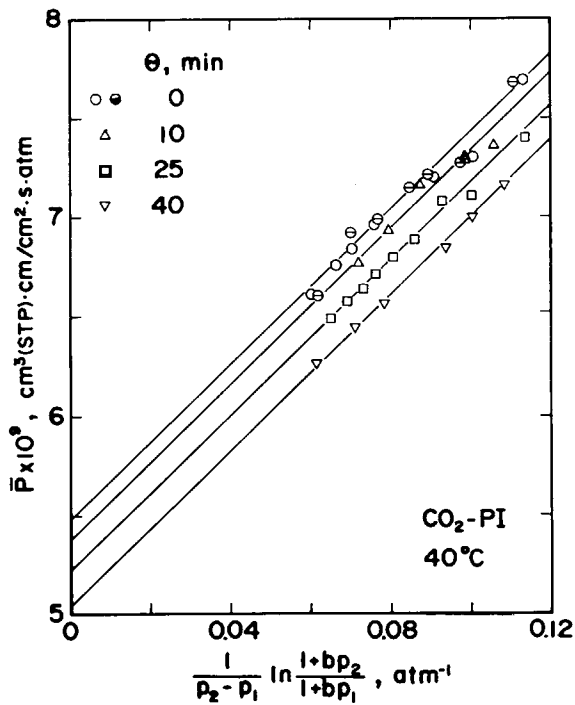


Fig. 16. Test of dual-mode mobility model driven by gradients of chemical potential for CO_2 -oxygen-plasma treated PI film at different durations (min) of treatment: (\circ , \ominus) 0; (Δ) 10; (\square) 25; (∇) 40.

Then, the permeability coefficient data for untreated and treated PI films were plotted on the basis of eq. (3). Figure 16 represents such plots. The plots for untreated and treated films give essentially straight lines and are therefore consistent with eq. (3). From the plot for an untreated film, D_D and D_H are estimated to be 8.42×10^{-8} and $8.37 \times 10^{-9} \text{ cm}^2/\text{s}$, respectively. For the sake of comparison, the present permeability data at 40°C were plotted on the basis of eqs. (2) and (3) using the value of b reported by Chern et al.¹¹ ($b = 0.32 \text{ atm}^{-1}$) in Figure 17. In this case, also, the dual-mode mobility model driven by gradients of chemical potential works well. Further, all straight lines in Figure 16 are found to be parallel, which implies that the diffusion coefficient of Langmuir mode, D_H , is independent of plasma exposure time. From the intercepts of the straight lines, the diffusion coefficients of Henry's law mode, \bar{D}_D , defined in eq. (12), were determined for different durations of treatment. In Figure 18, the ratio of the diffusion coefficient for a treated film to that for an untreated film was plotted against duration of treatment. For a 40-min oxygen-plasma-treated PI film, \bar{D}_D is reduced by 8%.

The pressure dependencies of the mean permeability coefficients of H_2 in oxygen-plasma-treated PI films are shown in Figure 19. Also, the permeabilities are found to be independent of upstream pressure, following eq. (14). By use of this equation, the diffusion coefficients of Henry's law mode (\bar{D}_D) were determined. The ratio of \bar{D}_D for a treated film to that for an untreated film was also plotted against duration of treatment in Figure 18. The effect of

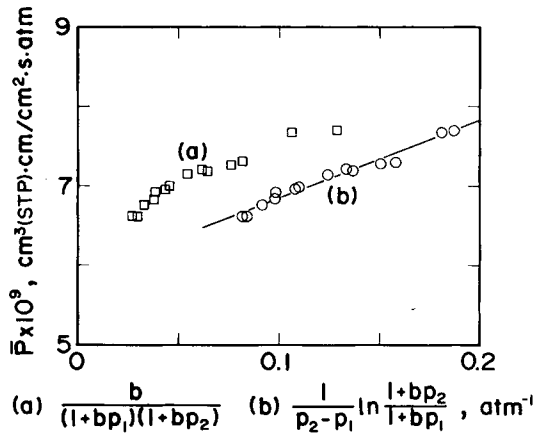


Fig. 17. Test of dual-mode mobility model using the Langmuir affinity constant reported by Chern et al.¹¹

plasma treatment on PI films upon the process of diffusion of Henry’s law mode for H₂ and CO₂ is found to be same. This is attributable to a more rigid structure of base polymer. Therefore, the oxygen-plasma treatment on PI films is not successful for improved permselectivity.

Permeabilities of CO₂ and H₂ in Ar-Plasma-Treated PSF Films

Measured permeability coefficients of CO₂ through Ar-plasma-treated PSF films were plotted on the basis of eq. (3) in Figure 20. The plots for treated as well as untreated films exhibited straight lines in parallel with each other. Accordingly, the dual-mode mobility model driven by gradients of chemical potential works well, and, besides, the diffusion coefficient of Langmuir mode, D_H, is independent of duration of Ar-plasma treatment. The effect of oxygen-

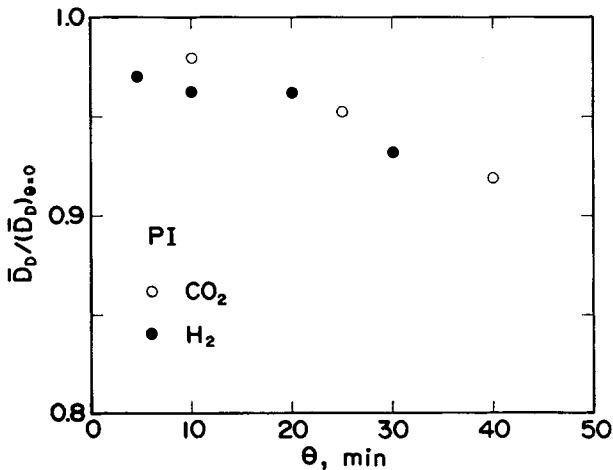


Fig. 18. Effect of duration of treatment on diffusion coefficients of CO₂ (○) and H₂ (●) in oxygen-plasma treated PI film.

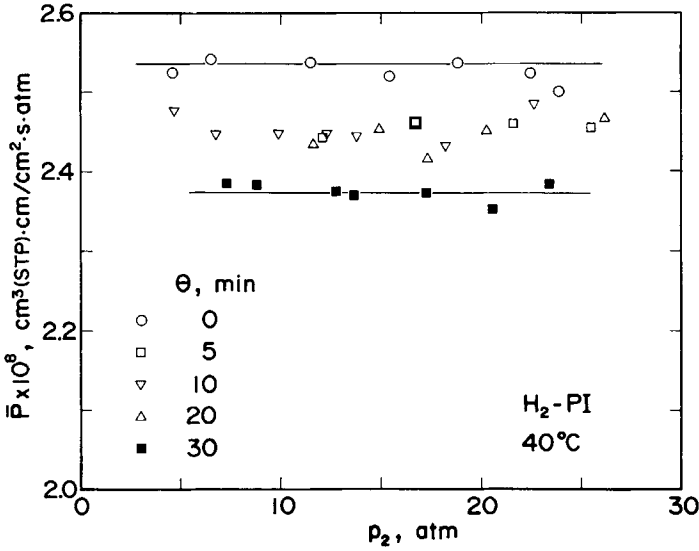


Fig. 19. Permeability coefficients for H₂ in PI film with and without oxygen-plasma treatment. θ (min): (○) 0; (□) 5; (▽) 10; (△) 20; (■) 30.

plasma treatment for a duration of 20 min is equivalent to that of Ar-plasma treatment for 10 min. Figure 21 illustrates the pressure dependence of the mean permeability coefficients of H₂ in Ar-plasma-treated PSF films. Also, the permeability is found to be, regardless of upstream pressure, consistent with eq. (14). In Figure 22, the ratios of the diffusion coefficients of Henry's law mode for CO₂ and H₂ in treated films to those in untreated films were plotted against the duration of Ar-plasma treatment. A 20-min treatment

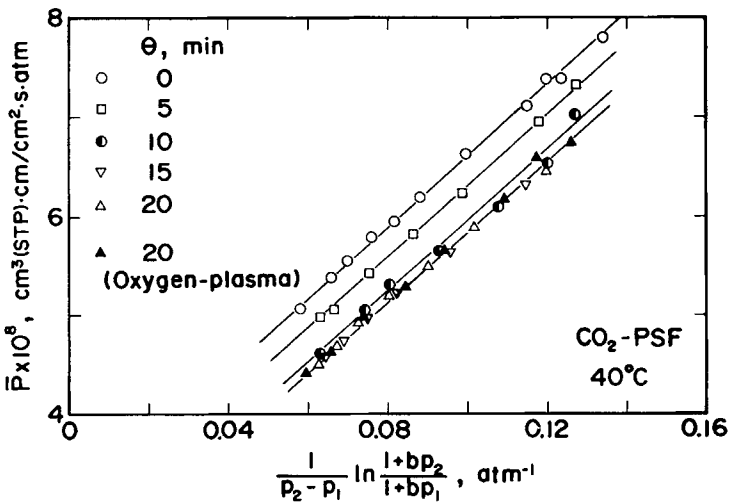


Fig. 20. Test of dual-mode mobility model driven by gradients of chemical potential for CO₂-Ar-plasma treated PSF film at different durations (min) of treatment: (○) 0; (□) 5; (●) 10; (▽) 15; (△) 20; (▲) 20.

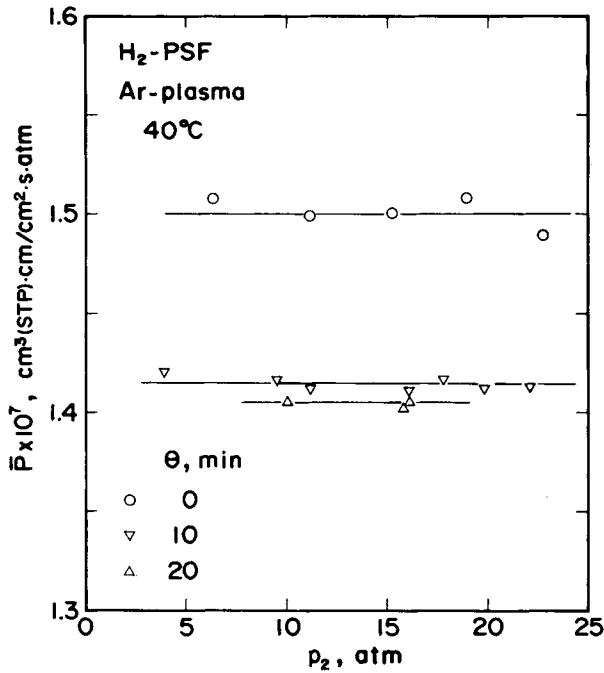


Fig. 21. Permeability coefficients of H₂ in PSF film with and without Ar-plasma treatment. θ (min): (○) 0; (▽) 10; (△) 20.

induced 26% reduction of CO₂ diffusivity compared to only 6% reduction of H₂ diffusivity. Hence, the Ar-plasma treatment on PSF films can improve permselectivity of H₂ relative to CO₂.

The surface modification by oxygen- and Ar-plasma treatment on PSF films appears to be efficient for improvement of permselectivity of H₂. This may be attributable from the fact that a crosslinked thin layer is formed on the surface of the polymer film.

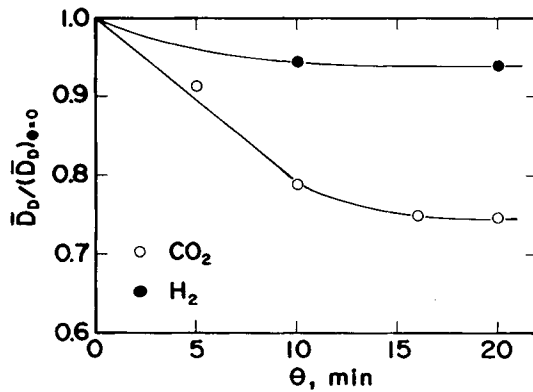


Fig. 22. Effect of duration of treatment on diffusion coefficients of CO₂ (○) and H₂ (●) in Ar-plasma treated PSF film.

CONCLUSION

The sorption equilibria and permeation behavior for CO₂ in PSF and PI films are simulated well by the dual-mode sorption and mobility model. For these systems, the dual-mode mobility model works better in terms of gradients of chemical potential rather than concentration. The sorption equilibria for H₂ in both films are described well by Henry's law, and the permeabilities are independent of applied pressure.

The oxygen- and Ar-plasma treatment on PSF and PI films apparently induces a reduction of only the diffusivity of Henry's law population, while the diffusivity of the Langmuir population is apparently not influenced by plasma treatment. The diffusivity of Henry's law mode for CO₂ in PSF films is reduced more than that for H₂ by plasma treatment. The effect of oxygen-plasma treatment on PI films upon a reduction of diffusivity of Henry's law mode for CO₂ and H₂ is almost the same. The surface modification by oxygen- and Ar-plasma treatment on PSF films appears to be successful for improved permselectivity of H₂ relative to CO₂.

APPENDIX: NOMENCLATURE

- b Langmuir affinity constant (atm⁻¹)
- C total sorbed concentration [cm³(STP)/cm³]
- C_D concentration of Henry's law population [cm³(STP)/cm³]
- C_H concentration of Langmuir population [cm³(STP)/cm³]
- C_H' Langmuir capacity constant [cm³(STP)/cm³]
- D diffusion coefficient in polymer film (cm²/s)
- D' diffusion coefficient in plasma treated layer (cm²/s)
- \bar{D}_D mean diffusion coefficient of Henry's law population defined in eq. (12) (cm²/s)
- J_s steady-state diffusion flux [cm³(STP)/(cm² s)]
- k_D Henry's law constant [cm³(STP)/(cm² atm)]
- l thickness of polymer film (cm)
- l_1 thickness of base-polymer layer (cm)
- l_2 thickness of plasma-treated layer (cm)
- \bar{P} mean permeability coefficient [cm³(STP) cm/(cm² s atm)]
- \bar{P}_1 mean permeability coefficient in base-polymer layer [cm³(STP) cm/(cm² s atm)]
- \bar{P}_2 mean permeability coefficient in plasma-treated layer [cm³(STP) cm/(cm² s atm)]
- p_1 downstream pressure (atm)
- p_2 upstream pressure (atm)
- p_i pressure in between plasma-treated and base-polymer layers as depicted in Figure 10 (atm)

Greek symbol

- ⊖ duration of plasma treatment (min)

Subscripts

- D Henry's law mode
- H Langmuir mode

References

1. D. R. Paul and W. J. Koros, *J. Polym. Sci., Polym. Phys. Ed.*, **14**, 675 (1976).
2. J. H. Petropoulos, *J. Polym. Sci., Polym. Phys. Ed.*, **8**, 1797 (1970).
3. E. Sada, H. Kumazawa, H. Yakushiji, Y. Bamba, K. Sakata, and S.-T. Wang, *Ind. Eng. Chem. Res.*, **26**, 433 (1987).

4. W. J. Koros, D. R. Paul, and A. A. Rocha, *J. Polym. Sci., Polym. Phys. Ed.*, **14**, 687 (1976).
5. S. A. Stern, P. J. Gareis, T. F. Sinclair, and P. H. Mohr, *J. Appl. Polym. Sci.*, **7**, 2935 (1963).
6. J. H. Hollahan and A. T. Bell, *Techniques and Applications of Plasma Chemistry*, Wiley, New York, 1974, p. 61.
7. E. Sada, H. Kumazawa, P. Xu, and M. Nishigaki, *J. Membr. Sci.*, **37**, 165 (1988).
8. A. J. Erb and D. R. Paul, *J. Membr. Sci.*, **8**, 11 (1981).
9. Y. Maeda and D. R. Paul, *J. Polym. Sci., Polym. Phys. Ed.*, **25**, 957 (1987).
10. D. R. Paul, *Ber. Bunsenges. Phys. Chem.*, **83**, 294 (1979).
11. R. T. Chern, W. J. Koros, B. Yui, H. B. Hopfenberg, and V. T. Stannett, *J. Polym. Sci., Polym. Phys. Ed.*, **22**, 1061 (1984).

Received May 12, 1988

Accepted August 15, 1988